PARTICLE SIMULATION OF COHESIVE GRANULAR MATERIALS

HANS-GEORG MATUTTIS

hg@acolyte.t.u-tokyo.ac.jp, Department of Applied Physics, School of Engineering, The University of Tokyo, Bunkyo-ku, Tokyo 113, Japan

and

ALEXANDER SCHINNER

schinner@acm.org, Institut for theoretical and computational Physics, University of Magdeburg, PF 4120 D-39106 Magdeburg, Germany

Received (received date)
Revised (revised date)

Abstract

We present two-dimensional molecular dynamics simulations of cohesive regular polygonal particles. The cohesive part of the force-law for the particle-particle interaction is validated by the agreement with existing experimental data. We investigate microscopic parameters which are not accessible to experiments such as contact length, raggedness of the surface and correlation time. With increasing cohesion the particles move in clusters for long times.

1. Introduction

In recent years, interest in the effects of cohesion in granular materials has increased [2, 3, 10, 13]. Experimental observations suggests that for increasing cohesion strength the behaviour of grains changes from movement of independent particles to a movement of small clusters. In this paper, we investigate the effects related to this correlated movement of cohesive particles. In Refs. [2, 3, 10], the angle of repose of

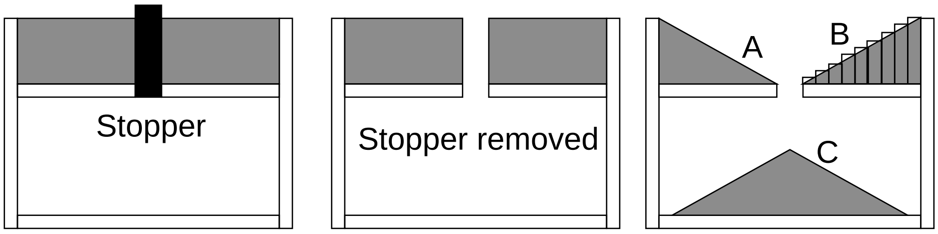

Figure 1: Draining-crater method to measure the angle of repose for granular materials. For region B, the histogram to measure the area under the slope is shown. The width of the bars was smaller than the particle size.

a pile of cohesive granular material was measured via the "draining-crater method", [5] where a box is filled with cohesive grains, and emptied via a narrow outlet in the middle, see Fig. 1. The angle of repose in the regions A and B (see Fig. 1) depends linearly on the strength of the cohesion. Cohesion effects can be caused by the surface properties of grains even without mesoscopic aggregates of fluid. This can be seen from the slow time-dependent increase of static friction in grains [13], crystal surfaces [18], and rocks [7], caused by the humidity of the surrounding air, which leads

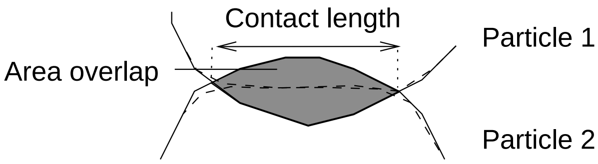

Figure 2: Undeformed (full line) and deformed (dashed line) particles in a contact. The force resulting from the deformation is assumed to be proportional to the area overlap of the colliding particles. The penetration depth is exaggerated in comparison to simulations with realistic parameters.

to interstices on a nanometric scale. Whether the cohesion is due to the wetting fluid outside the particle contact zones, which has been argued in Refs. [2, 3, 10], or whether most of the liquid is concentrated around the contact zones, as argued in Refs. [9, 14] is not relevant for our modelization.

2. Simulation method

To model and numerically simulate cohesion as a feature of the contacts, we used the discrete element method. It is based on molecular dynamics, where the particle trajectories are computed according to Newton's equation of motion. In our simulation, the particles are represented by polygons. The force between two particles is proportional to the Young's modulus and to the overlap area (representing the deformation) of two polygons. Additionally, damping in normal direction and friction in tangential direction is implemented. More details of the force law for the contact- and damping forces are explained in [15]. The simulation was performed for a two-dimensional system. We assumed that the cohesion strength is proportional to the contact area. Then, for two dimensions, the force is proportional to the contact length (dotted line) whereas the repulsive force was chosen [15] proportional to the area overlap of two particles (shaded region in Fig. 2). For spheres, the area overlap A and penetration depth x are proportional as $A \propto x^{3/2}$. That means if regular polygons with a large number of corners are used in the simulation, they are interacting via a Hertzian contact law. No rolling friction was implemented, because no coefficients are available in the literature for granular materials, and the normal dissipations dampens away rotations anyway, depending on the number of corners used.

As parameters we chose the cohesion strength k_{coh} with units [N/m] in two dimensions, so that the attractive force F_{coh} is proportional to the contact length l:

$$F_{\mathrm{coh}} = k_{\mathrm{coh}} \cdot |l|, \tag{0.1}$$

In contrast to the model used in Ref. [12] for polygons, where the attractive force acts between the centres of mass of the particles, in our model the cohesive force acts at the contact points and depends on the length of the particle contact. The contact points are chosen as the centre of the intersection points. Choosing alternatively the contact point as the centre of mass of the overlap polygon resulted not in any significant changes. Our definition of the cohesive force in Eq. 0.1 can be implemented easily in a simulation of polygons where the whole geometry of the contact is known. In the case of round particles, where only the penetration depth is computed, more complicated expressions are derived for the cohesion, see Ref. [11].

In our simulations of the draining crater method, where the maximum force results from 10-40 particle layers, the average contact length (see Fig. 3) of the particles increased linearly with the cohesion strength k_{coh}. The area of overlap of

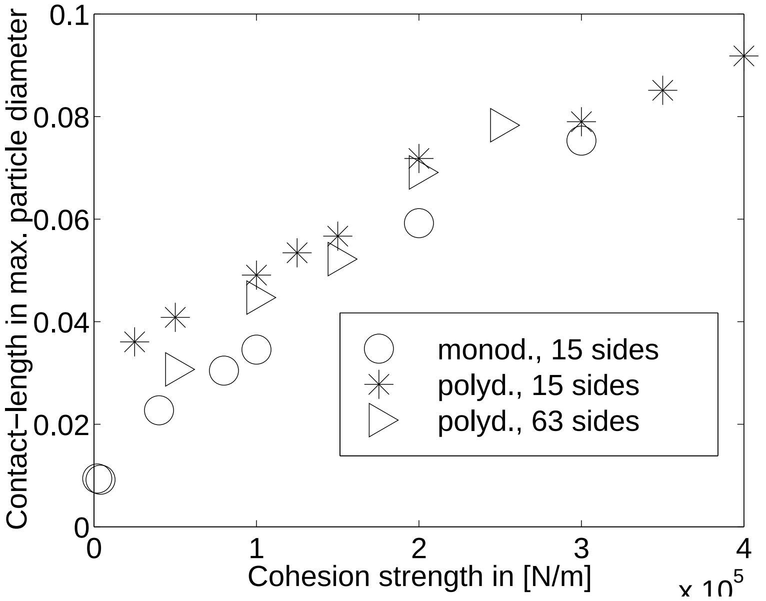

Figure 3: Contact length of neighbouring particles

the particles (not shown) increases also linearly. A contact length of 0.01–0.1 particle diameters as in Fig. 3 corresponds to a penetration depth of between 0.00025 and 0.00251 particle diameters for circles, 4-3 orders of magnitudes less than the particle diameter. This is in accord with the thickness of the "coating layer" of oil which was reported to be less than 4 orders of magnitude of the particle radius in the experiments [2]. This justifies neglecting the volume of the cohesive layer as we did to derive the cohesive force purely from the contact length.

In the simulation, the static and dynamic friction coefficients were chosen as $\mu_{\text{stat.}} = \mu_{dyn.} = 0.6$, Young's modulus was $Y = 10^7$ N/m, the particle diameter was 1 mm for the monodisperse, and 0.6-1 mm for the polydisperse particles. The time step for the simulations was dt$=0.2 \cdot 10^{-5}$ s, the density was 5000 kg/m^2.

3. Simulation geometry

The simulation was performed on a "draining-crater" in two dimensions which had about the same diameter in terms of the particle diameter as the experiment.The box size in the experiments [2, 3, 10] was about 80-250 particle diameters, in our simulation it was about 160-200 particle diameters. The size of the outlet was about 12-25 particles in the experiment and 12-40 particles in the simulation. One series of measurements was taken with monodisperse regular polygons with 15 faces, one series with a polydisperse mixture, and a linear distribution of the radius within the interval $[0.75 \cdot r, 1.25 \cdot r]$. Another series was taken with the same size dispersion, but with regular polygons with 63 faces to monitor the effect of size dispersion and particle shape. All series give consistent data for medium to strong cohesion. For weak cohesion, the monodisperse grains have a strong tendency to order on a triangular grid which dominates the entire physics of the system.

The forcelaw for the interaction between particles and floor/walls was the same as between particles, i.e. the same modulus of elasticity, cohesion and friction were chosen for simplicity.

We computed the angle of repose ϕ by calculating the two dimensional analogue from Ref. [10] so that

$$\tan\phi = 2 \cdot \frac{\text{area}}{\text{base length}^2}, \tag{0.2}$$

The advantage of calculating ϕ from the area below the slope is that it yields an integral criterion. This smoothes out any effects from jagged surfaces of the slopes, which are typical for strongly cohesive materials such as in Fig. 5. Different layers of the grains during initialisation of the particles are denoted by different shadings. For non cohesive materials like in Fig. 4, the angle of repose could also be computed using the tangent of the slope. Differential criteria for ϕ, e.g. via the local inclination of the slope become ambiguous for increasing cohesion, and additional averaging or smoothing is necessary.

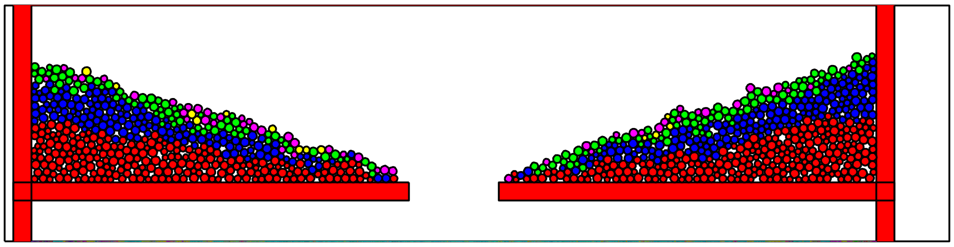

Figure 4: Smooth surface for weakly cohesive particles with cohesion parameter $k_{\text{coh}} = 0.5 \cdot 10^4$ N/m.

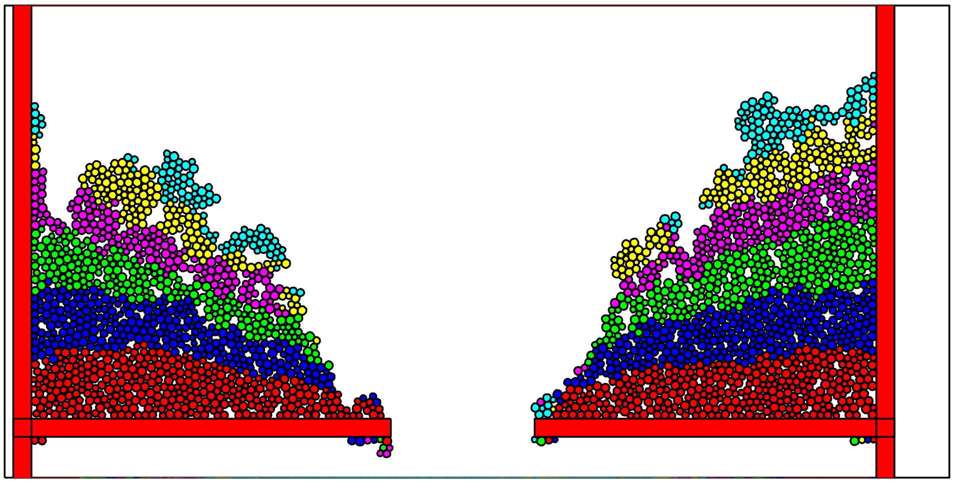

Figure 5: Ragged surface of a static configuration for strongly cohesive particles with cohesion parameter $k_{\text{coh}} = 3.5 \cdot 10^5$ N/m.

4. Angle of repose and additional lengthscales

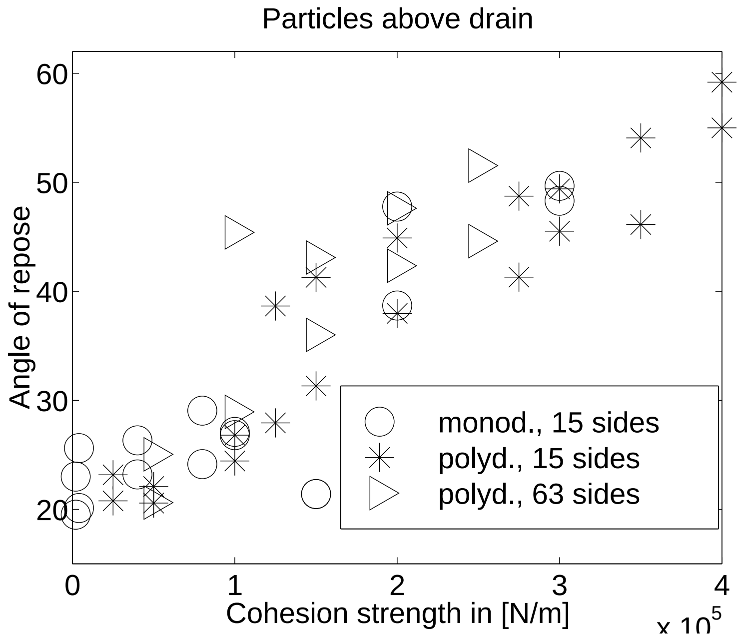

Figure 6: Angle of repose versus strength of the cohesion for the particles above the drain in regions A and B in Fig. 1.

Fig. 6 shows the angle of repose for the regions A and region B of Fig. 1. The scattering of the data is comparable with the experimental literature, see Refs. [2, 3, 10, 14]. The angle of repose for vanishing cohesion is consistent with the measurements in Ref. [10] for the dry granulates, with an angle of repose for dry material of about 20-23 degrees. Therefore, the minimum angle of repose in Refs. [10, 14] was the same as in our simulation.

Fitting the simulation data with experimental paper has some intrinsic difficulties. Whereas dry cohesive materials can be scaled easily, the cohesion introduces and additional length scale in the simulation. This is, loosely speaking, due to the fact that the cohesion, the force which keeps the heap together, increases with the surface area l^2 of a volume element of linear dimension l. In contrast, the shear force exerted by the weight of the volume element is proportional to l^3. This why cohesive slopes "fail in depth". Therefore, the critical angle for non-cohesive slopes is the same as cohesive slopes, a result which was published recently in Ref. [9], but has been textbook knowledge in geotechnics along with the continuum mechanics derivation for decades [17]. This is the strange case that probably the largest sand heaps on earth, the valleys of the yellow River in China, made of "cohesive" material, defy the thermodynamic limit. It was therefore not our intention to obtain simulations for any thermodynamic limit, but to establish that our simulation method can reproduce the phenomenology of the experiment under the dependence of a single parameter.

As far as our simulation are concerned, this means that we can compare only with experiments where the systems size in terms of particle diameters is comparable to our simulation, which is the case for Ref. [10], but not for for Ref. [14]. An increase of the average coating layer of 1 nm oil corresponds to an increase of the cohesion strength of 0.05 N/m for rods of 1 m length with 1 mm diameter. In region C in Fig. 1 the angle of repose (see Fig. 7) was found to be smaller than in regions A and

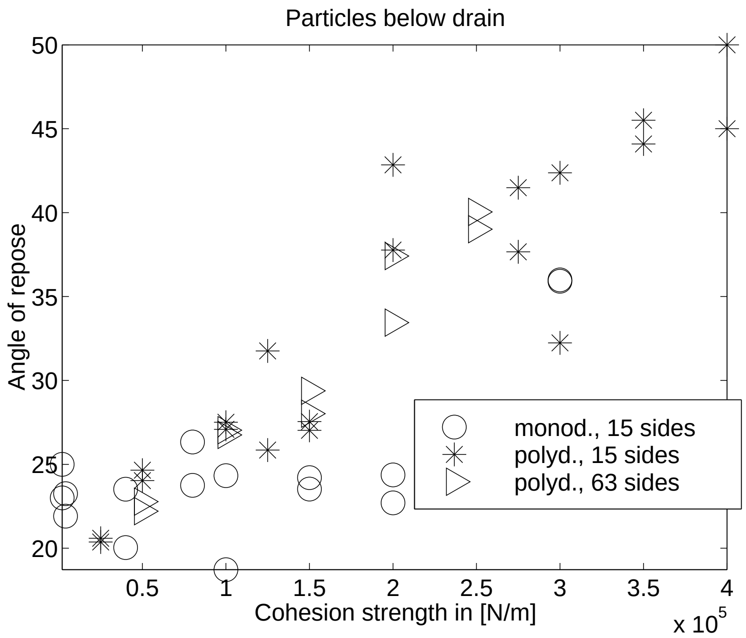

Figure 7: Angle of repose versus strength of the cohesion for the particles below the drain in region C of Fig. 1.

B of Fig. 1. This is probably due to the finite kinetic energy of the particles leaving the outlet. The area of the granular profile was computed via a histogram of the heap outline, see Fig. 1. This method was also employed for the ragged outline. Using the convex hull around the heap gave results with much larger data scattering in the strongly cohesive regime due to the jagged surface.

5. Clogging

Cohesion increases the tendency of flowing granules to clog in narrow outlets. If the cohesive force is strong enough ($k_{\rm coh} > 2 \cdot 10^5$N/m), an outlet of the diameter of 15-20 particles width clogs up easily, see Fig 8 (left). The cohesion is strong enough to glue the particles on to the bottom of the outlet. For non-cohesive material, the characteristic diameter for clogging outlets in simulation is about 5-6 particles. If for the clogged configuration, the cohesion is reduced to $k_{\rm coh} = 0$, the particles started flowing again, see Fig. 8 (right). This is a first indication of clustering of particles for strong cohesion. For outlets of the width of 20-25 particle diameters, no clogging was observed.

We made no systematic study of the clogging diameters, but as far as we can tell from these and other simulation in a different setup, the clogging seems to depend only on the width of the outlet, not on any external parameters like the depth of the sand layer above the outlet. In connection with other simulations, we filled a hopper with particles, and the clogging occurred at roughly the same particle-to-outlet ration, even without additional layers of sand. Due to arching, the

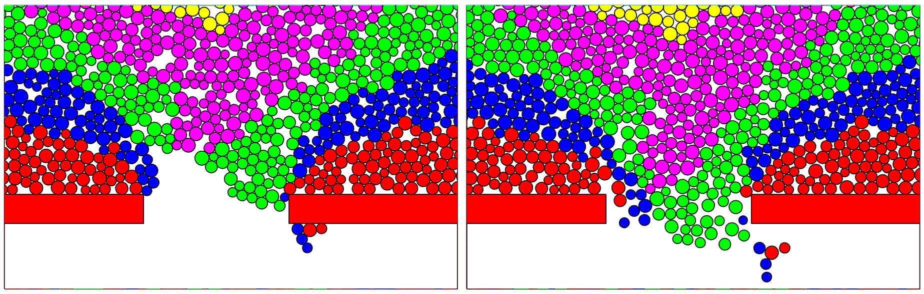

Figure 8: Left: Static configurations after clogging of an outlet with cohesion $k_{\rm coh} = 3.5 \cdot 10^5$N/m. Right: The same outlet with the same configuration of particles, after the cohesion has been "switched off" (right).

information about how deep the layer above the outlet is seems to get lost quickly.

6. Number of contacts

Up to here, the effects could also be derived from experiments, for the microscopic level (thickness of the cohesive layer/penetration depth) as well as for the macroscopic level (angle of repose, clogging) and therefore serve to validate the simulation. We will now turn to the measurements which are difficult or impossible to perform in experiments. These are original results which can only be obtained by simulations on the particle level.

For monodisperse systems, the average number of contacts, as shown in Fig. 9, is always near to 4, because these systems usually order on triangular lattices. Nevertheless, configurations are possible where the number of contacts deviates strongly from 4. For polydisperse systems, the number of contacts is proportional to the cohesion. From the available data, we could not decide whether the increase of the number of contacts with the increase of the cohesion is necessary for the stability of the increasing angle of repose. It might be possible that particles are simply glued together without carrying any static load as in the configuration in Fig. 8 (left).

7. Macroscopic surface shape

We investigated the "raggedness" of the slope depending on the cohesion. The difference between dry, smooth slopes in Fig.4 and cohesive, rough slopes in Fig.5 is obvious. To quantify this property, we subtracted the straight slope (computed from ϕ computed in Eq. 0.2) from the real slope and from the data computed the power spectrum. For the graph in Fig. 10, the data from region A and region B in Fig. 1 were averaged. It can be seen that the raggedness of the slopes increases strongly with the cohesion on all length-scales up to the length scale of the system, see Fig. 10. This shows that the clustering is continuous on the surface. In general, up to a cohesion strength of $k_{\rm coh} = 0.5 \cdot 10^5$N/m the heap properties do not deviate significantly from non-cohesive materials, like in Figs. 6, 11 and 10. However, this regime is possibly difficult to observe experimentally, because there is always a finite humidity in the air. If the air above the grains is completely dry, the drying process may take weeks, whereas if the grains are dried before they are used in the experiment, statics will influence the outcome of the whole experiments [4]. We therefore propose a measurement of the critical angle of oiled lead or bronze balls, which should be neither subject to magnetic nor electrostatic forces, so that experiments without spurious influences even in very dry environments should be

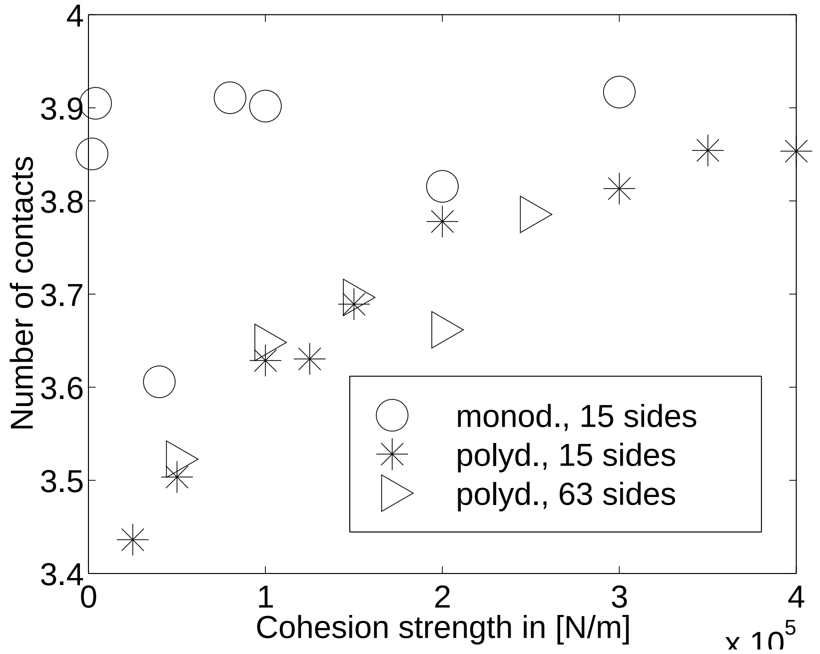

Figure 9: Average number of contacts, averaged over regions A, B and C in Fig. 2.

possible. Under these conditions, it should be possible to observe the range of constant critical angle for the range corresponding to 0 to $k_{\mathrm{coh}} = 0.5 \cdot 10^5 \mathrm{N/m}$.

8. Correlation between particles

The time correlation between particles (Fig. 11) was measured as the percentage of particles which were in contact at the time the stopper was blocking the outlet and at the end of the simulation. The data indicates that for increasing cohesion, particles move in clusters for long times. The graph also shows quantitatively that mixing is stronger in non-cohesive than in cohesive materials.

This indicates an increased correlation time between neighbouring particles, and the suppression of mixing of particles, because the particles are "chained together" by the cohesive forces.

We also measured the percentage of particles which were nearest neighbours and next nearest neighbours at the beginning and not more than 1 particle diameter distant at the end of the simulation, and the graphs are qualitatively the same, although more noisy.

From the increase of the correlation time for short range in the bulk and from the increase of the raggedness on all length scales on the surface in the previous section we conclude that the size of the clusters of moving particles increases continuously with the strength of the cohesion. We found no indication of a separation in "tight short range correlation" and "weak long range correlation".

The strong interparticle connection is reminiscent of simulations of non-spherical particles made from connected round particles [8]. In powder technology, the strength of the cohesion is classified by a single parameter together with the surface roughness

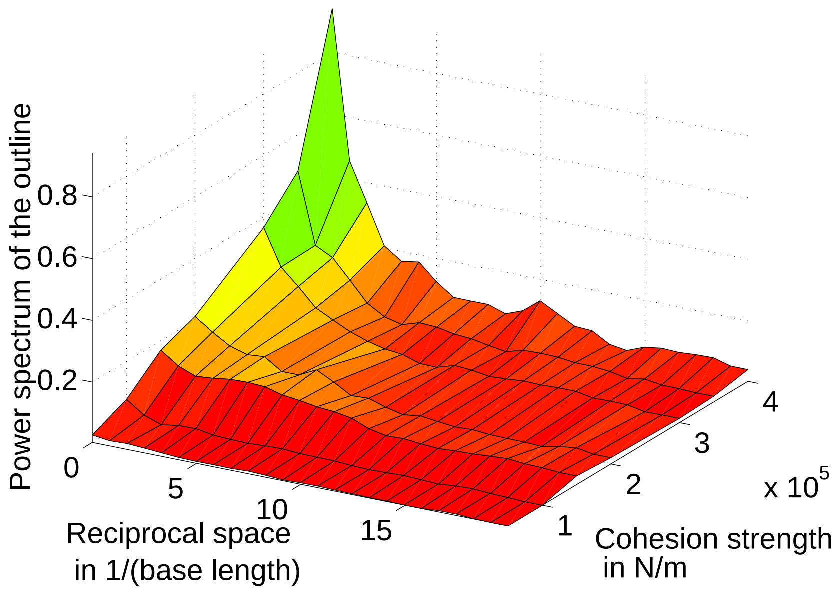

Figure 10: Power spectrum of the heap outline to determine the "raggedness" of a slope data of the regions A and B in Fig. 2 averaged. The units of reciprocal space are given in (1/l), where l is the base length of region A,B in Fig. 1.

of the grains. This parameter is independent of the angle of repose, as proposed by Carr [6] see e.g. Ref. [1]. The fact that the static friction for bulk solids can be independent of the particle roughness is already mentioned in the textbook by Rabinowicz [16]. Increasing the friction alone is not sufficient for increasing the angle of repose of a heap, because at some limit angle, the particles will start to roll, the heap 'fails on the surface'. In contrast, with roughness or cohesion, the rotational degree of freedom can be efficiently blocked and the angle of repose can be increased almost indefinitely. Also, cohesion alone is not able to prevent a particle from sliding down a smooth slope, if no static friction is present. These arguments mean that roughness/cohesion is distinct from friction. As cohesion and particle roughness cannot be distinguished by macroscopic parameters, we propose our modelling of cohesion also to mimic an effective "roughness" of grains in computer simulations without implementing additional geometric information for the particles.

9. Summary

We showed that the inclusion of cohesion, together with static friction and contact forces, was sufficient to model cohesive granular materials on the micro-scale so that the full range of macroscopic effects could be reproduced by the simulation and a good agreement with experimental data was obtained. No systematic deviations between the three-dimensional experimental data and the two dimensional simulation data were encountered. Using this agreement as validation, measurements of the correlation time, the contact number and the surface raggedness of the slope were presented. All three parameters indicate that the size of clusters increases continuously with the cohesion. Further investigations will be necessary

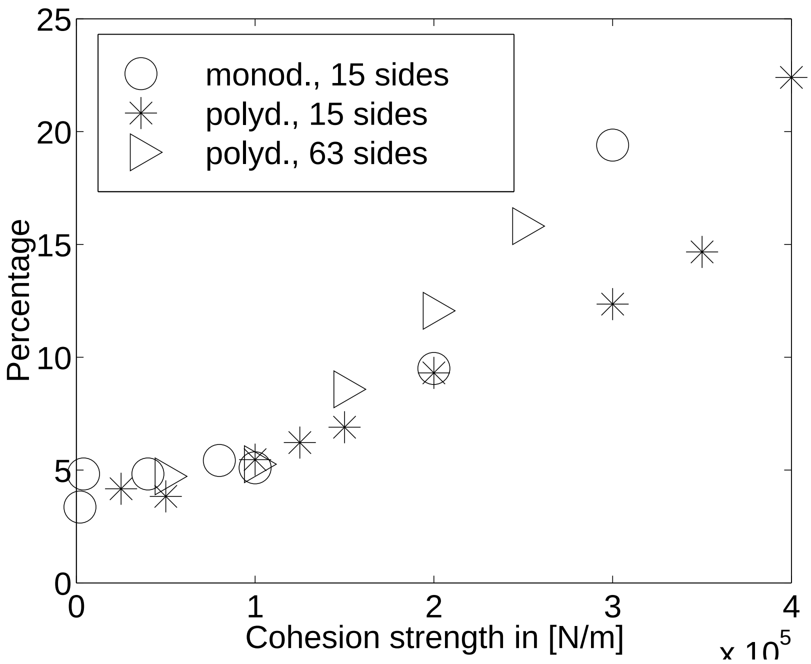

Figure 11: Percentage of particles which were nearest neighbours at the start of the simulation and were still in contact at the end of the simulation in region C in Fig. 2 .

to obtain a better statistical description of the clusters. The authors are indebted to L. Barabasi and P. Schiffer for inspiring and stimulating the work and offering additional information as well as to K. Kassner, K. Aoki and F. Kun for helpful discussions. We also thank the NIC in Jülich for the grant to use their T3E supercomputers.

1. T. Akiyama and Y. Tanijiri. Criterion for re-entrainment of particles. *Powder Technology*, 57:21–26, 1989.
2. R. Albert, I. Albert, D. Hornbaker, P. Schiffer, and A.-L. Barabási. Maximum angle of stability in wet and dry spherical granular media. *Phys. Rev. E*, 56(6):R6271–R6274, 1997.
3. R. Albert, M. A. Pfeifer, and A.-L. Barabási. Drag force in a granular medium. 1998.
4. K. Aoki. private communication.
5. R. L. Brown and J. C. Richards. *Principles of Powder mechanics*. Pergamon, Oxford, 1970.
6. R. L. Carr. *Journ. Chem. Engin.*, 18:163, 1965.
7. J. Dieterich and G. Conrad. Effect of humidity on time- and velocity-dependent friction in rocks. *J. Geophysical Research*, 89:4196–4202, 1984.
8. J. A. C. Gallas and S. Sokołowski. Grain non-sphericity effects on the angle of repose of granular material. *Int. J. of Mod. Phys. B*, 7(9 & 10):2037–2046, 1993.
9. Thomas C. Halsey and Alex J. Levine. How sandcastles fall. *Phys Rev Letters*, 80(14):3141–3144, 1998.

10. D. J. Hornbaker, R. Albert, I. Albert, A.-L. Barabasi, and P. Schiffer. What keeps sandcastles standing? *Nature*, 387:765, 1997.
11. K.L. Johnson, K. Kendall, and A.D. Roberts. Surface energy and the contact of elastic solids. *Proc. R. Soc. Lond. A*, 324:301–313, 1971.
12. Ferenc Kun and Hans J. Herrmann. Transition from damage to fragmentation in collision of solids. *Phys. Rev. E*, 59(3):2623–2632, 1999.
13. L.Bocquet, E.Charlaix, S.Ciliberto, and J.Crassous. Moisture induced aging in granular media and the kinetics of capillary condensation. *Nature*, 396:745–737, 1998.
14. T.G. Mason, A.J. Levine, D. Erats, and T. C. Halsey. Critical angle of wet sandpiles. *Phys Rev E*, 60:R5044–R5047, 1999.
15. H.-G. Matuttis. Simulations of the pressure distribution under a two dimensional heap of polygonal particles. *Granular Matter*, 1(2):83–91, 1998.
16. Ernest Rabinowicz. *Friction and Wear of Materials*. John Wiley, New York, London, Sidney, 1965.
17. P. Vermeer. Personal communication using his lecture notes from his student days at the end of the 1960's.
18. J.H Westbrook and P.J Jorgensen. Effect of water desorption on indentation microhardness anisotropy in minerals. *The American Mineralogist*, 53:1899–1914, 1968.